Intermediate-band solar cells based on quantum dot supracrystals

Q. Shao and A. A. Balandin[a)]
Nano-Device Laboratory, Department of Electrical Engineering, University of California-Riverside, Riverside, California 92521, USA

A. I. Fedoseyev and M. Turowski
CFD Research Corporation, Huntsville, Alabama 35805, USA

(Received 1 September 2007; accepted 24 September 2007; published online 16 October 2007)

The authors show that the ordered three-dimensional arrays of quantum dots, i.e., quantum dot supracrystals, can be used to implement the intermediate-band solar cell with the efficiency exceeding the Shockley-Queisser limit for a single junction cell. The strong electron wave function overlap resulting in minibands formation allows one to tune the band structure and enhance the light absorption and carrier transport. A first-principles semianalytical approach was used to determine the optimum dimensions of the quantum dots and the interdot spacing to achieve a maximum efficiency in the $InAs_{0.9}N_{0.1}/GaAs_{0.98}Sb_{0.02}$ quantum dot supracrystal photovoltaic cells. © *2007 American Institute of Physics*. [DOI: 10.1063/1.2799172]

The energy conversion efficiency is a key parameter in the photovoltaic (PV) solar cell technology. It is defined as

$$\eta = \frac{FFV_{oc}J_{sc}}{P_{in}}, \tag{1}$$

where FF is the fill factor, V_{oc} is the open circuit voltage, J_{sc} is the short-circuit current density, and P_{in} is the incident power per unit area. The performance of the conventional bulk semiconductor cells is limited to about 33%.[1] The theoretical thermodynamic limit on the conversion of sunlight to electricity is much higher, about 93%.[2] Thus, there is a very strong motivation for finding new approaches, which would allow one to increase the solar cell efficiency.

Luque and Marti[3] have theoretically shown that introduction of the intermediate energy level between the valence band (VB) and conduction band (CB) of a regular semiconductor can increase the efficiency up to ~63%. Unlike VB and CB, the third energy level—intermediate band (IB)—is not directly electrically contacted, although the radiative transitions between IB and two other bands are allowed.[3,4] IB helps to harvest photons with an energy less than the band gap of host material via a two-step process, which allows one to improve the short-circuit current without degrading the open-circuit voltage.[3–8]

Practically, IB can be created through the introduction of an impurity band in regular bulk semiconductors, e.g., similar to the earlier proposal by Wolf,[9] or formation of a miniband in a superlattice-type structure.[4] The difficulty of the IB approach is how to practically obtain the required exact energy spacing among all three bands.[3,5,10] The original proposal of the PV efficiency enhancement via IB and the work that followed assumed that all optimum bands and energy separations are given.[3,5,10] No semiconductor superlattice structure with exactly defined parameters, which would allow one to implement the IB approach, has so far been specified.

In this letter, we show that a quantum dot superlattice (QDS) with three-dimensionally (3D) ordered quantum dots can provide the electron and hole energy dispersion, which are suitable for implementing the IB solar cell, and find the exact parameters of QDS required to operate in the IB regime. We consider 3D-ordered QDS with the closely spaced quantum dots and high quality interfaces, which allow for the strong wave function overlap and the formation of minibands.[11] In such structures, the quantum dots play a role similar to that of atoms in real crystals. To distinguish such nanostructures from the disordered multiple arrays of quantum dots, we refer to them as quantum dot *supracrystals*. There have already been a number of reports of 3D-ordered QDS (Refs. 12–15) as well as in-plane two-dimensionally ordered (Refs. 16 and 17) and vertically one-dimensionally ordered (Ref. 18) QDSs. One should expect that further progress in epitaxial growth and self-assembly will deliver more ordered QDS with closely spaced quantum dots. Previous studies confirm the formation of minibands in QDS (Ref. 19) similar to those in quantum well superlattices (QWS).

A schematic of the considered supracrystal structure with the periodically arranged quantum dots is shown in Fig. 1. QDS is sandwiched between p and n type layers. IB has to be half-filled with electrons which could be achieved by modulation doping at the barrier region.[6] By engineering the QDS parameters such as quantum dot size, shape, interdot separation, and dot arrangement, one can optimize IB position and width to achieve the maximum efficiency. The first step for demonstrating a possibility of forming optimum

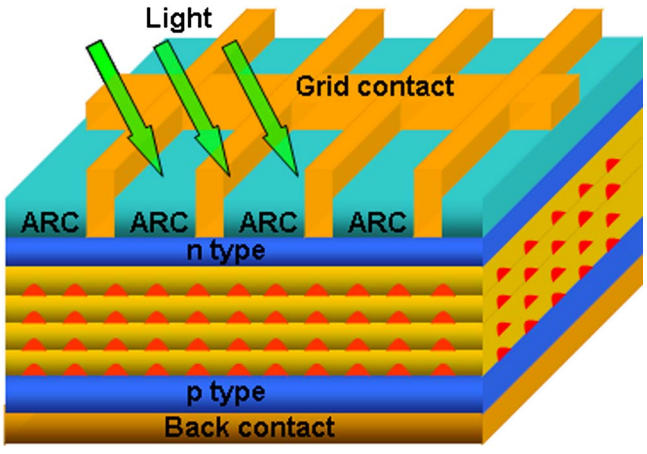

FIG. 1. (Color online) Schematic of the quantum dot supracrystal solar cell.

[a)]Author to whom correspondence should be addressed. Electronic mail: balandin@ee.ucr.edu. URL: http://www.ndl.ee.ucr.edu/

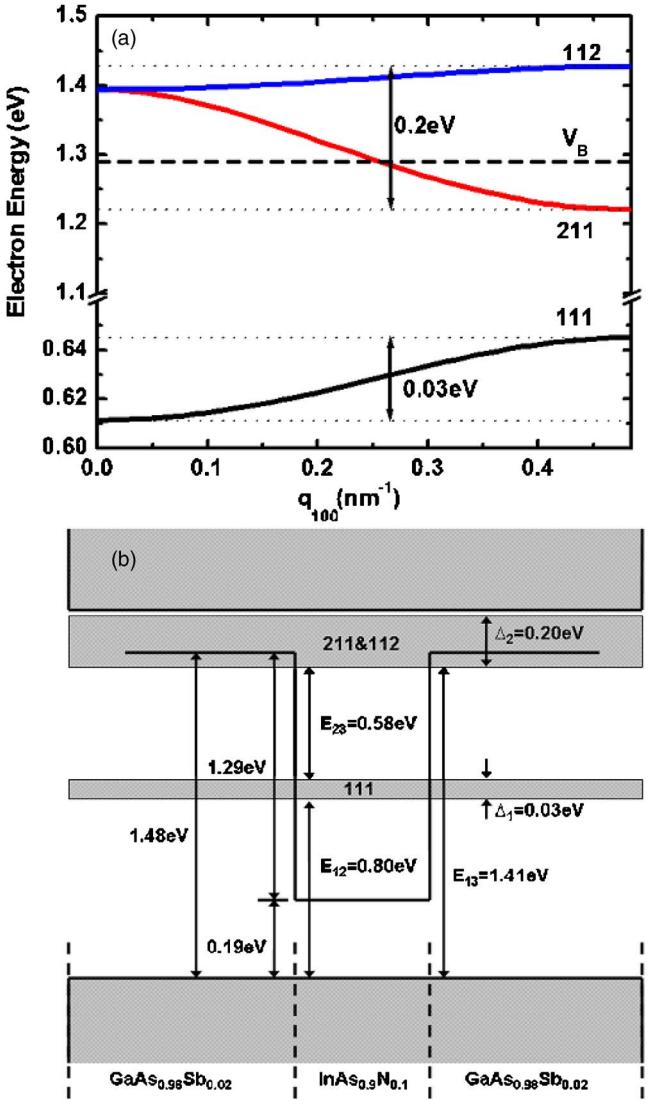

FIG. 2. (Color online) (a) Electron dispersion in $InAs_{0.9}N_{0.1}/GaAs_{0.98}Sb_{0.02}$ quantum dot supracrystal along the [[100]] quasicrystallographic direction. Results are shown for the simple cubic QDS with the quantum dot size $W=4.5$ nm and interdot spacing $H=2$ nm along all directions. The energy in units of eV is counted from the bottom of the potential well. (b) Energy diagram showing minibands formed in the same structure.

IB is to calculate the electron dispersion in such structure by solving the Schrödinger equation. It has been accomplished following the Lazarenkova and Balandin[11] semianalytical approach, which gives the solution for 3D-ordered QDS through the Kronig-Penny-type expression. The accuracy of this semianalytical solution has been later verified by the finite-element simulations.[19,20]

We performed 3D analysis on an example of QDS made of $InAs_{0.9}N_{0.1}/GaAs_{0.98}Sb_{0.02}$ material system. The valence band offsets are negligible in this system and the conduction band offset is equal to $E_{\text{barrier}} \approx 1.29$ eV.[21] The values for the electron effective masses, $m^*_{\text{InAsN}}=0.0354m_0$ and $m^*_{\text{GaAsSb}}=0.066m_0$ (m_0 is the electron rest mass), and other band parameters have been taken from Ref. 22. Figure 2(a) shows the calculated electron energy dispersion $E(q)$ in the simple cubic (SC) QDS with the quantum dot size $W=4.5$ nm and the interdot distance $H=2$ nm. The minibands are labeled by the quantum numbers n_x, n_y, and n_z, which define the total energy of an electron as the sum of its component along three axes.[11] The dispersion is shown for the electron wave vector q along [[100]] quasicrystallographic direction in the coordinate system formed by the quantum dots in the supracrystal (we retained the notations proposed by Lazarenkova and Balandin[11,19]). The [[100]] direction is the most important one since it defines the charge carrier transport in the vertical direction (see Fig. 1) to n and p type layers.

One can see from Fig. 2(a) that the bandwidth of the minibands are 0.03 eV for the band 111 and 0.2 eV for the overlapping minibands 211 and 112. The higher-index minibands whose energies are higher than E_{barrier} are mutually overlapping or very close to each other. For these reasons, we consider the higher-energy minibands as a quasicontinuum CB. In Fig. 2(b), we depict the real-space band diagram for our prototype structure with the calculated energies and miniband widths. Here, the miniband 111 acts as IB, while the overlapping minibands 211 and 112 act as the band analogous to CB from where the generated electrons are extracted as a current flow. The VB in our structure is the same as in bulk semiconductors owing to the small VB offset.

The values of W and H, which led to the dispersion and band diagram shown in Figs. 2(a) and 2(b) are not arbitrary. They were chosen after simulating the electron energy dispersion as those which give the transition energies $E_{13}=1.41$ eV, $E_{23}=0.58$ eV, $E_{12}=0.80$ eV, and the IB (miniband 111) width $\Delta_1=0.03$ eV. These energy separations between CB and IB and between IB and VB are very close to those determined by Levy *et al.*[21] for the same material system. Assuming as given the optimum energy band parameters ($E_{13}=1.48$ eV, $E_{23}=0.51$ eV, $E_{12}=0.97$ eV, and $\Delta_1=0$), Levy *et al.*[21] calculated the maximum IB solar cell efficiency of ~60.5%. Thus, we have demonstrated that SC arrangement of quantum dots in the supracrystal is versatile enough to provide the miniband, which acts as IB and lead to the efficiency enhancement.

The theoretical limit for the PV efficiency of IB solar cell determined in Ref. 21 has been calculated for the idealized band structure with the zero IB width ($\Delta_1=0$) and optimum E_{23} of 0.51 eV. In our case, all band parameters are defined by the actual electron dispersion in QDS and cannot be tuned independently. For these reasons, E_{23} and Δ_1 slightly deviate from the optimum values. In order to determine the PV efficiency of our supracrystal with IB, we follow the detailed balance theory of Shockley and Queisser.[23] The calculations are performed under the standard assumptions of the ideal solar cell specified by Luque and Marti,[3] i.e., nonradiative transitions are forbidden, the quasi-Fermi levels are constant throughout the whole cell volume, PV cell is thick enough to assure full absorption of the photons with enough energy to induce any of the transitions depicted in Fig. 2, and Ohmic contacts are applied in such a way that only electrons (holes) can be extracted from the conduction (valence) band to form the external current.

For an ideal solar cell, the photon-generated current is proportional to the difference between the number of photons absorbed by the device and the number of photons emitted from the device. In the IB solar cell, the short-circuit current density J_{SC} can be written as[3]

$$J_{\text{SC}}/q = [\dot{N}(E_{13},\infty,T_s,0) - \dot{N}(E_{13},\infty,T_a,\mu_{CV})] + [\dot{N}(E_{23},E_{12},T_s,0) - \dot{N}(E_{23},E_{12},T_a,\mu_{CI})], \quad (2)$$

where T_s is the temperature of the Sun (6000 K), T_a is the

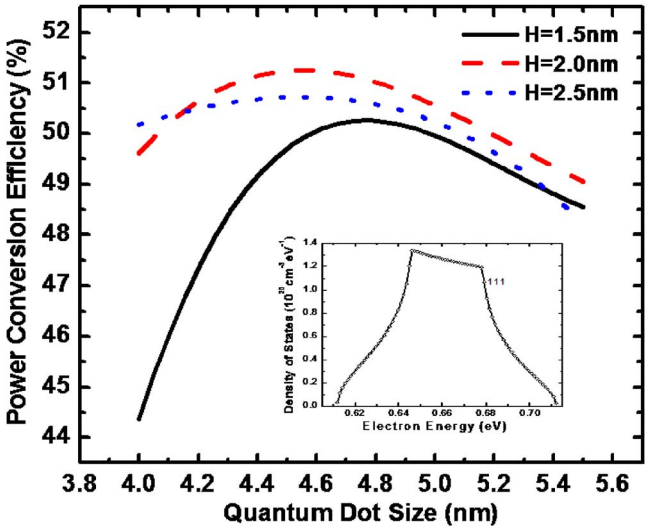

FIG. 3. (Color online) Photovoltaic power conversion efficiency as a function of the quantum dot size in $InAs_{0.9}N_{0.1}/GaAs_{0.98}Sb_{0.02}$ quantum dot supracrystal. The results are shown for several interdot separations. The inset shows the electron density of states in the miniband 111, which serves as an intermediate band in the supracrystal solar cell. The structure parameters are the same as in Figs. 1 and 2.

temperature of the solar cell (300 K), $\dot{N}$ is the flux of photons absorbed by or emitted from the semiconductor, and E_{13}, E_{23}, E_{12} are specified in Fig. 2(b). In thermodynamic equilibrium, $\dot{N}$ is given by[24]

$$\dot{N}(E_l,E_h,T,\mu) = \frac{2\pi}{h^3c^2}\int_{E_l}^{E_h} \frac{E^2 dE}{e^{(E-\mu)/k_BT}-1}, \tag{3}$$

where E_l and E_h are the lower and upper energy limits of the photon flux for the corresponding transitions, respectively, μ is the chemical potential of the transition, k_B is Boltzmann constant, E is the photon energy, h is Planck constant, and c is the speed of light. The output voltage can be described as the difference of the chemical potentials between CB and VB, i.e., $qV_{OC}=\mu_{CV}=\mu_{CI}+\mu_{IV}$ (for the considered system, $\mu_{CI}=0.53$ eV and $\mu_{IV}=0.80$ eV).

Assuming that in Eq. (1) the fill factor is unity and the incident power is $P_{in}=\sigma T_s^4$ (here σ is the Stefan-Boltzmann constant), one can calculate the efficiency upper limit for the optimum QDS parameters. Figure 3 shows the PV power conversion efficiency of the IB solar cell based on quantum dot supracrystal as a function of the dot size. The maximum efficiency obtained for QDS with $W=4.5$ nm and $H=2$ nm, which has the band structure parameters close to the "ideal" ones, is 51.2%. It is smaller than the value obtained in Ref. 21 but still significantly larger than the Shockley and Queisser limit of ~30% for bulk semiconductors.[23]

The properties of IB itself deserve a special consideration. The electron density of states (DOS) in IB has to be as high as possible in order to pin the IB quasi-Fermi level at its equilibrium position.[8] We determined DOS per unit energy and per unit volume $G(E)$ as a function of the electron energy $E(q)$ from the equation

$$G(E) = \frac{2}{(2\pi)^3}\oint \frac{dS_E}{|\nabla_q E(q)|}, \tag{4}$$

where the integration is carried over the surface of constant energy S_E. DOS for IB (111 miniband) in the SC supracrystal is presented in the inset to Fig. 3. As one can see, DOS in QDS is very different from that in conventional QWS or bulk crystals. The area under the DOS curve is 7.395×10^{18} cm^{-3}, which is of the same order of magnitude as DOS in VB and CB and provides sufficient IB quasi-Fermi level pinning.

In conclusion, we determined the parameters of QDS required for implementation of the IB solar cell. Solar cells based on quantum dots may carry extra benefits of increased radiation hardness[25] and improved collection efficiency.[4,26]

This work has been supported by the AFOSR under Contract No. FA9550-07-C-0059 and by the NASA under Contract No. NNC07CA20C. The authors acknowledge insightful discussions with Dr. V. Mitin, Dr. K. Reinhardt, Dr. S.G. Bailey, and Dr. S. Hubbard.

[1] T. Tiedje, E. Yablonovitch, G. D. Cody, and B. G. Brooks, IEEE Trans. Electron Devices **ED-31**, 711 (1984).
[2] P. T. Landsberg and G. Tonge, J. Appl. Phys. **51**, R1 (1980).
[3] A. Luque and A. Marti, Phys. Rev. Lett. **78**, 5014 (1997).
[4] M. A. Green, in *Handbook of Semiconductor Nanostructures and Nanodevices*, Photovoltaic Applications of Nanostructures Vol. 4, edited by A. A. Balandin and K. L. Wang (ASP Stevens Ranch, California, 2006), pp. 219–237.
[5] M. A. Green, Nanotechnology **11**, 401 (2000).
[6] A. Marti, N. Lopez, E. Antolin, E. Canovas, C. Stanley, C. Farmer, L. Cuadra, and A. Luque, Thin Solid Films **511/512**, 638 (2006).
[7] S. Sinharoy, C. W. King, S. G. Bailey, and R. P. Raffaelle, *Proceedings of the 31st IEEE Photovoltaic Specialists Conference* (IEEE, New Jersey, 2005), pp. 94–97.
[8] L. Cuadra, A. Marti, and A. Luque, Thin Solid Films **451/452**, 593 (2004).
[9] M. Wolf, Proc. IRE **48**, 1246 (1960).
[10] A. S. Brown, M. A. Green, and R. P. Corkish, Physica E (Amsterdam) **14**, 121 (2002).
[11] O. L. Lazarenkova and A. A. Balandin, J. Appl. Phys. **89**, 5509 (2001).
[12] G. Springholz, V. Holy, M. Pinczolits, and G. Bauer, Science **282**, 734 (1998).
[13] Y. I. Mazur, W. Q. Ma, X. Wang, Z. M. Wang, G. J. Salamo, M. Xiao, T. D. Mishima, and M. B. Johnson, Appl. Phys. Lett. **83**, 987 (2003).
[14] S. Kiravittaya, M. Benyoucef, R. Zapf-Gottwick, A. Rastelli, and O. G. Schmidt, Appl. Phys. Lett. **89**, 233102 (2006).
[15] J. S. Kim, M. Kawabe, and N. Koguchi, Appl. Phys. Lett. **88**, 072107 (2006).
[16] A. A. Balandin, K. L. Wang, N. Kouklin, and S. Bandyopadhyay, Appl. Phys. Lett. **76**, 137 (2000).
[17] A. A. Balandin, G. Jin, and K. L. Wang, J. Electron. Mater. **20**, 549 (2000).
[18] J. L. Liu, W. G. Wu, A. A. Balandin, G. L. Jin, Y. H. Luo, S. G. Thomas, Y. Lu, and K. L. Wang, Appl. Phys. Lett. **75**, 1745 (1999).
[19] O. L. Lazarenkova and A. A. Balandin, Phys. Rev. B **66**, 245319 (2002).
[20] D. L. Nika, E. P. Pokatilov, Q. Shao, A. A. Balandin, Phys. Rev. B **76**, 125417 (2007).
[21] M. Y. Levy, C. Honsberg, A. Marti, and A. Luque, *Proceedings of the 31st IEEE Photovoltaic Specialists Conference* (IEEE, New Jersey, 2005), pp. 90–93.
[22] I. Vurgaftman, J. R. Meyer, and L. R. Ram-Mohan, J. Appl. Phys. **89**, 5815 (2001).
[23] W. Shockley and H. J. Queisser, J. Appl. Phys. **32**, 510 (1961).
[24] L. D. Landau and E. M. Lifchitz, *Physique Statistique* (Mir, Moscow, 1967), 206.
[25] F. Guffarth, R. Heitz, M. Geller, C. Kapteyn, H. Born, R. Sellin, A. Hoffmann, D. Bimberg, N. A. Sobolev, and M. C. Carmo, Appl. Phys. Lett. **82**, 1941 (2003).
[26] O. F. Yilmaz, S. Chaudhary, and M. Ozkan, Nanotechnology **17**, 3662 (2006).